Study on the Disturbance Rejection of Virtual Slope Walking by Stepper-2D Robot

Mingguo Zhao[1,2], HaoDong[1] and Naiyao Zhang[1]

[1]*State Key Laboratory of Robotics and System (HIT)*
[2]*Department of Automation, Tsinghua University, Beijing 100084, China*
(mgzhao@tsinghua.edu.cn, donghao00@mails.tsinghua.edu.cn, zlh@tsinghua.edu.cn)

Abstract: Virtual Slope Walking is a new realization of powered walking based on Passive Dynamic Walking, which is not only effective in generating fast walking, but also achieving advantages on disturbance rejection. Under the open-loop condition without external sensing device, the step-handling walking with maximum step height of 10% leg length is realized on a planar bipedal robot Stepper-2D. This paper theoretically studies the disturbance rejection of Virtual Slope Walking by introducing the ground step perturbation. We theoretically proved that the step perturbation can be transformed to the disturbance of initial system state and successful step handling walking comes from the system's cyclic stability. The necessary and sufficient condition of recovering from the step perturbation is obtained and confirmed by the experiment on Stepper-2D.

Keywords: **Bipedal robot; Virtual Slope Walking; Disturbance Rejection.**

I. INTRODUCTION

McGeer [1] demonstrated that a Passive Dynamic Walker can walk down a shadow slope with no control and actuation in the early of 1990. Then the concept of Passive Dynamic Walking has been used as a starting point for designing powered walkers to walk on level ground. Wisse[3], Hobbelen[4] and Collins[5]. demonstrated several realizations of powered walking based on kinematic energy complement. Asano [6], Honjo [7] and Harata [8] introduced the parametric excitation for potential energy restoration. In our previous work [9] [10], we proposed Virtual Slope Walking by introducing the leg length modulation and achieved a relative speed of 4.48leg/s on a planar bipedal robot Stepper-2D.

Disturbance rejection, defined as the ability to deal with unexpected disturbances [11], is considered as one of the fundamental performances for bipedal walking. There exists several ways to measure the disturbance rejection for a PDW based walker theoretically, such as Floquet multipliers, Basin of Attraction and the Gait Sensitivity Norm. But the most commonly used experimental measure is the ground step perturbation that a walker can handle without falling. Wisse[12] realized powered walking under a step height of 2% leg length disturbance. Pratt [13] realized powered walking under a step height of 9% leg length. Geng [14] achieved powered walking under a step height of 4% leg length by on-line machine learning and PDW based mechanism designed. We[15][16] have realized a powered walking under a step height of 10% leg length on Stepper-2D based on Virtual Slope Walking.

In this paper, we theoretically study the disturbance rejection of Virtual Slope Walking and present its stabilizing mechanism under. Based on the asymptotic expression of stride function and the fixed point, we theoretically proved that ground step perturbation can be transformed to the disturbance of initial system state and the successful step handling walking comes from the fixed point's stability. Then the necessary and sufficient condition of recovering from the step perturbation is presented based on the analysis of the relationship between the system state and the minimum initial state in the transition phase, providing the possibility to quantitatively analyze the maximal relative step height.

The remainder of this paper is organized as follows. In Section Ⅱ, the model of Virtual Slope Walking is presented. In Section Ⅲ, the ground step disturbance handling is illustrated, and the performance of disturbance rejection is analyzed in Section Ⅳ. Section Ⅴ presents the experimental results and Section Ⅵ the conclusion and future work.

II. Model of Virtual Slope Walking

1 Model Description

A cartoon of the Virtual Slope Walking model is shown in Fig. 1. We assumed that the model has two telescopic massless legs and a point mass body at the hip. The stance leg is actuated for extending from r_s to r_e following a smooth leg length trajectory r(t), the swing leg is actuated for shortening from r_e to r_s in one step. The length shorten ratio is then defined as $\beta=r_s/r_e$. Since the swing leg is assumed massless, it can be swung arbitrarily quickly to the position with constant inter-leg angle φ_0 before heel strike. The impact of the swing leg with the ground is assumed to be fully inelastic (no slip, no bounce) and instantaneous, which implies that there exists discontinues change in the velocity of the center of mass and unchanged system configuration.

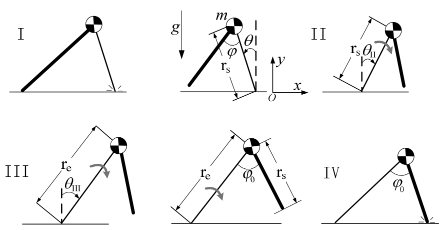

Fig. 1 Model of Virtual Slope Walking

We define a walking step starts when the new stance leg (lighter line) has just made contact with the ground in the upper left picture, namely instant I. The stance leg swings to the position at $\theta=\theta_{II}$ in the upper right picture for the beginning of extension, namely instant II. And the stance leg extension ends at $\theta=\theta_{III}$ in the bottom left picture, namely instant III. The swing leg (heavier line) is shortened and swings to the position with constant inter-leg angle φ_0 just before heel strike in the bottom middle picture, and hits the ground in the bottom right picture, namely instant IV. Then, the stance leg and swing leg exchange subsequently, and the walking cycle repeats continuously.

2 Governing Equations

The governing equations of the system consist of nonlinear differential equations for the swing phase and algebraic equations for the transitions of heel strike.

(1) Swing phase from **I** to **II**: Using *Lagrangian Equations*, the second-order differential equation of motion is given below for the swing phase of the stance leg with the constant length r_s under the dimensionless time variable $\tau = \sqrt{g/r_e}\,t$

$$\ddot{\theta}(\tau) = \frac{1}{\beta}\sin\theta(\tau) \tag{1}$$

For the simplicity, we will refer to dimensionless time τ as the time variable, henceforward.

(2) Stance leg extension From **II** to **III**: The stance leg acts as an inverted pendulum with variable length $r(\tau)$. Using the *Lagrangian Equations*, the equation of motion can be written as

$$\begin{cases} \ddot{\theta}(\tau) = \dfrac{r_e}{r(\tau)}\sin\theta(\tau) - \dfrac{2}{r(\tau)}\dot{r}(\tau)\dot{\theta}(\tau) \\ \ddot{r}(\tau) = r(\tau)\dot{\theta}^2(\tau) - r_e\cos\theta(\tau) + r_e\dfrac{F}{mg} \end{cases} \tag{2}$$

where F is the force that the leg exert on the center of mass during the stance leg extension.

(3) Swing phase from **III** to **IV**: Similar to the equation in Eq. (1), the equation of motion for the stance leg with the constant length r_e can be written as

$$\ddot{\theta}(\tau) = \sin\theta(\tau) \tag{3}$$

(4) Heelstrike transition from **IV** to **I** of the subsequent step: The heelstrike from step n to the subsequent step n+1 occurs when the geometric collision condition

$$\begin{cases} \theta_{\mathrm{I}}(n+1) = -(\varphi_0 - \theta_{\mathrm{IV}}(n)) \\ \beta\cos\theta_{\mathrm{I}}(n+1) = \cos\theta_{\mathrm{IV}}(n) \end{cases} \tag{4}$$

is met, where the '**I**' and '**IV**' subscripts denote the instant **I** and **IV** respectively, φ_0 is the constant of the inter-leg angle at heels trike. Eq. (4) also reflects a change of names for the two legs. The swing leg becomes the stance leg, and vice versa.

From the conservation of angular momentum about the swing foot contact point at heel strike, we obtain the following transition equation

$$\omega_{\mathrm{I}}(n+1) = \frac{\cos\varphi_0}{\beta}\omega_{\mathrm{IV}}(n) \tag{5}$$

Eq. (1)-(5) construct the dynamic equations of this hybrid system.

3 Stride Function and Fixed Point

The general procedure for the study of this model is based on interpreting a step as a Poincaré map, or, as McGeer termed it, a 'stride function' [1]. Our Poincaré section is at the start of a step, namely instant **I** in Fig. 1. Given the state of the system at instant **I**, the Poincaré map **f** determines the state just after the next heelstrike. Note that in the geometric collision condition Eq. (4), the stance leg angle θ_I is constant with inter-leg angle φ_0

$$\theta_{\mathrm{I}} = -\arctan\frac{\beta - \cos\varphi_0}{\sin\varphi_0} \tag{6}$$

So the heels trike transition reduces this problem in 2D state space $\{\theta_I, \omega_I\}$ to a one dimensional map **f**, only consisting of angular velocity ω_I. So, while the system has only one independent initial condition, we need to specify ω_I at the start of walking step n to fully determine the subsequent motion at steps n+1, n+2,… so that $\omega_I(n+1)$ can be obtained from $\omega_I(n)$ by the Poincaré mapping. We have proved that under the **Equivalent Definition**, The Trajectory Leg Extension (TLE) can be equivalently transformed to the Instantaneous Leg Extension (ILE) [15] in Virtual Slope Walking. Consequently, defining a new variable $q=\omega^2_I$ as the system state, the stride function **f** can be analytically obtained under the Instantaneous Leg Extension (ILE) as follows

$$\begin{aligned} \mathbf{f}(q) &= \beta^2\cos^2\varphi_0 q \\ &+2\cos^2\varphi_0[\cos\theta^*_{\mathbf{II}}(\frac{1}{\beta^2} - \beta) - \cos\theta_{\mathbf{I}}(\frac{1}{\beta} - \beta)] \end{aligned} \tag{7}$$

where θ^*_{II} is the equivalent extension angle. Since the walking with TLE and its equivalent ILE produces the equivalent cyclic walking motion, ILE can be used as a theoretical tool for the analysis of Virtual Slope Walking without the dependence on numerical simulation.

The fixed point of the stride function is defined as $\mathbf{f}(q^f) = q^f$. From Eq. (7), the fixed point can then be obtained as follows

$$q^f = \frac{2\cos^2\varphi_0[\cos\theta^*_{\mathbf{II}}(1-\beta^3) - \cos\theta_{\mathbf{I}}(\beta-\beta^3)]}{\beta^2(1-\cos^2\varphi_0\beta^2)} \tag{8}$$

III. Ground Step Disturbance Handling

1. Transition Walking

After entering into the periodic state in Virtual Slope Walking, once the system is perturbed by a single step, there will be a transition phase in the subsequent one or two walking steps. And after that, the system state will approach the fixed point asymptotically the same as the condition of initial state's disturbance in Virtual Slope Walking. We will illustrate such transition walking by introducing the single step-up and step-up-down perturbations in the following section.

The Sixteenth International Symposium on Artificial Life and Robotics 2011 (AROB 16th '11),
B-Con Plaza, Beppu,Oita, Japan, January 27-29, 2011

2. Single Step-Up Perturbation

We assume that the system is in the periodic state in step n-2, and a single step-up perturbation occurs at the end of step n-1, just at heel strike. The subsequent transition walking step n is shown in Fig. 2. In the transition phase, there exist the perturbations not only on the system state q, but also on the stance leg angle θ_{I} and θ_{IV}, which is constant in normal walking, resulting in the variation of the stride function. After the transition phase ends, only disturbance on the system state q exists.

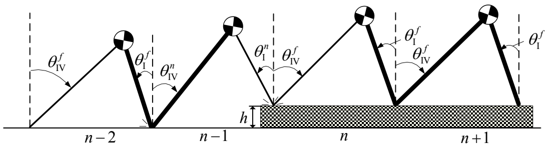

Fig. 2 Transition Walking of the Single Step-Up Perturbation

Let h be the step disturbance height, and $h_r=h/r_e$ be the relative value. Then, the perturbation on the stance leg angle θ_{I} and θ_{IV} resulted from the step height disturbance in the transition walking step n can be obtained as follows

$$\begin{cases} \theta_{\mathrm{IV}}^{n} + \theta_{\mathrm{I}}^{n} = \varphi_0 \\ \cos\theta_{\mathrm{IV}}^{n} = \beta\cos\theta_{\mathrm{I}}^{n} + h_r \end{cases} \tag{9}$$

The system state at the start of step n can be considered as the output of the stride function with perturbed θ_{IV} of step n-1. Let θ^f_{I} and θ^f_{IV} be the constant stance leg angle which is corresponded to the fixed point, then $q(n)$ can be represented as

$$\begin{aligned} q(n) &= \beta^2\cos^2\varphi_0 q^f \\ &\quad +2\cos^2\varphi_0[\cos\theta_{\mathrm{II}}^{*}(\frac{1}{\beta^2}-\beta)-(\frac{1}{\beta^2}\cos\theta_{\mathrm{IV}}^{n}-\beta\cos\theta_{\mathrm{I}}^{f})] \end{aligned} \tag{10}$$

There exists the perturbation on θ_{I} in transition walking step n (Fig. 2), so q(n+1) can be considered as the output of the stride function with perturbed θ_{I} of step n

$$\begin{aligned} q(n+1) &= \beta^2\cos^2\varphi_0 q(n) \\ &\quad +2\cos^2\varphi_0[\cos\theta_{\mathrm{II}}^{*}(\frac{1}{\beta^2}-\beta)-(\frac{1}{\beta^2}\cos\theta_{\mathrm{IV}}^{f}-\beta\cos\theta_{\mathrm{I}}^{n})] \end{aligned} \tag{11}$$

θ_{I} and θ_{IV} returns to the constant value from step n+1, then q(n+2) can be represented as

$$\begin{aligned} q(n+2) &= \beta^2\cos^2\varphi_0 q(n+1) \\ &\quad +2\cos^2\varphi_0[\cos\theta_{\mathrm{II}}^{*}(\frac{1}{\beta^2}-\beta)-\cos\theta_{\mathrm{I}}^{f}(\frac{1}{\beta}-\beta)] \end{aligned} \tag{12}$$

The transition phase ends after step n, and the system state starts approaching the fixed point asymptotically with the initial state of $q(n+1)$.

It can be concluded from Eq. (10)&(11) that the single step-up perturbation introduces the disturbance on the system state q of step n and transfers such disturbance by the stride function in the subsequent transition phase. It is indicated from Eq. (12) that after the transition phase ends, the step perturbation can be totally transformed to the disturbance of initial system state. So, once the continuous walking condition of the initial state is satisfied, the system state will definitely approach the fixed point in the following walking steps.

3. Single Step-Up-Down Perturbation

We assume that the system is in the periodic state in step n-2, and a single step-up-down perturbation occurs at the end of step n-1, just at heel strike. The subsequent transition walking steps n and n+1 are shown in Fig. 3. The same as the step-up perturbation, in the transition phase, there exist the perturbations not only on the system state q, but also on the stance leg angle θ_{I} and θ_{IV}, which is constant in normal walking, resulting in the variation of the stride function. After the transition phase ends, only disturbance on the system state q exists.

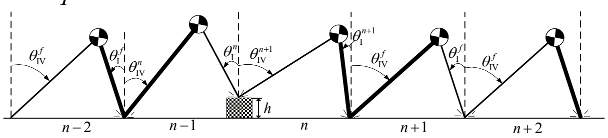

Fig. 3 Transition Walking of the Single Step-Up-Down Perturbation

The perturbation on the stance leg angle θ_{I} and θ_{IV} resulted from the step height disturbance in the transition walking step n and n+1 can be obtained as follows

$$\begin{cases} \theta_{\mathrm{IV}}^{n} + \theta_{\mathrm{I}}^{n} = \varphi_0 \\ \cos\theta_{\mathrm{IV}}^{n} = \beta\cos\theta_{\mathrm{I}}^{n} + h_r \end{cases}, \begin{cases} \theta_{\mathrm{IV}}^{n+1} + \theta_{\mathrm{I}}^{n+1} = \varphi_0 \\ \cos\theta_{\mathrm{IV}}^{n+1} = \beta\cos\theta_{\mathrm{I}}^{n+1} - h_r \end{cases} \tag{13}$$

The system state at the start of step n can be considered as the output of the stride function with perturbed θ_{IV} of step n-1. So $q(n)$ can be represented as

$$\begin{aligned} q(n) &= \beta^2\cos^2\varphi_0 q^f \\ &\quad +2\cos^2\varphi_0[\cos\theta_{\mathrm{II}}^{*}(\frac{1}{\beta^2}-\beta)-(\frac{1}{\beta^2}\cos\theta_{\mathrm{IV}}^{n}-\beta\cos\theta_{\mathrm{I}}^{f})] \end{aligned} \tag{14}$$

Both perturbations on θ_{I} and θ_{IV} exist in transition walking step n (Fig. 5), so q(n+1) can be considered as the output of the stride function with perturbed θ_{I} of step n and θ_{IV} of step n+1

$$\begin{aligned} q(n+1) &= \beta^2\cos^2\varphi_0 q(n) \\ &\quad +2\cos^2\varphi_0[\cos\theta_{\mathrm{II}}^{*}(\frac{1}{\beta^2}-\beta)-(\frac{1}{\beta^2}\cos\theta_{\mathrm{IV}}^{n+1}-\beta\cos\theta_{\mathrm{I}}^{n})] \end{aligned} \tag{15}$$

There exists the perturbation on θ_{I} in transition walking step n+1 (Fig. 3), so $q(n+2)$ can be considered as the output of the stride function with perturbed θ_{I} of step n+1

$$\begin{aligned} q(n+2) &= \beta^2\cos^2\varphi_0 q(n+1) \\ &\quad +2\cos^2\varphi_0[\cos\theta_{\mathrm{II}}^{*}(\frac{1}{\beta^2}-\beta)-(\frac{1}{\beta^2}\cos\theta_{\mathrm{IV}}^{f}-\beta\cos\theta_{\mathrm{I}}^{n+1})] \end{aligned} \tag{16}$$

θ_{I} and θ_{IV} returns to the constant value from step n+2, then q(n+3) can be represented as

$$\begin{aligned} q(n+3) &= \beta^2\cos^2\varphi_0 q(n+2) \\ &\quad +2\cos^2\varphi_0[\cos\theta_{\mathrm{II}}^{*}(\frac{1}{\beta^2}-\beta)-\cos\theta_{\mathrm{I}}^{f}(\frac{1}{\beta}-\beta)] \end{aligned} \tag{17}$$

The transition phase ends after step n+1, and the system state starts approaching the fixed point asymptotically with the initial state of q(n+2).

It can be concluded from Eq. (14)-(16) that the single step-up-down perturbation introduces the same disturbance as that of the single step-up perturbation. It is indicated from Eq. (17) that after the transition phase ends, the step perturbation can be totally transformed to the disturbance of initial system state. The only difference is that the transition phase of single step-up-down perturbation includes one more step than that of single step-up perturbation. So, once the continuous walking condition of the initial state is satisfied, the system state will also definitely approach the fixed point in the following walking steps.

So we can draw the conclusion from the above results that the step height perturbation can be totally transformed to the disturbance of initial system state, and the disturbance rejection problem in Virtual Slope Walking can be transformed to the stabilizing problem of the fixed point if the continuous walking condition is satisfied.

Ⅳ Analysis of Disturbance Rejection of Virtual Slope Walking

1. Maximum Relative Step Height

There exists the maximum relative step height h_r^{max} when $q(n)=q^z(n)$ holds as h_r increases, which describes the performance of disturbance rejection of Virtual Slope Walking. Therefore, h_r^{max} can be obtained as follows

$$h_r^{\max} = \beta \tan^2\varphi_0 \cos\theta_{\mathrm{I}}^n + \begin{cases} \frac{1}{2}\beta^4 q^f + \cos\theta_{\mathrm{II}}^*(1-\beta^3) + \beta^3\cos\theta_{\mathrm{I}}^f - \dfrac{\beta}{\cos^2\varphi_0}, \theta_{\mathrm{II}}^* > 0 \\ \frac{1}{2}\beta^4 q^f + \dfrac{1-(1-\beta^3)(1-\beta^2\cos^2\varphi_0)\cos\theta_{\mathrm{II}}^*}{\beta^2\cos^2\varphi_0} + \beta^3\cos\theta_{\mathrm{I}}^f, \theta_{\mathrm{II}}^* \le 0 \end{cases} \tag{18}$$

where h_r^{max} and θ_I^n satisfy

$$\begin{cases} \theta_{\mathrm{IV}}^n + \theta_{\mathrm{I}}^n = \varphi_0 \\ \cos\theta_{\mathrm{IV}}^n = \beta\cos\theta_{\mathrm{I}}^n + h_r^{\max} \end{cases} \tag{19}$$

It can be concluded from Eq. (18)&(19) that the maximum relative step height h_r^{max} is determined by the model parameters length shorten ratio β, equivalent extension angle θ^*_{II} and inter-leg angle φ_0. We will illustrate the influence of model parameters on the disturbance rejection in the following section.

2. Influence of Model Parameters

2.1 Effect of the Length Shorten Ratio β

The maximum relative step height hrmax is shown as a function of β in Fig.4 with four values of φ0. It is indicated from Fig.4 that hr^{max} decreases with an increase in β. An increase in β causes a net decrease in the extended leg length, resulting in a decrease in the complementary energy E_c and a decrease in the system kinematic energy which is represented by the system state q. On the other side, an increase in β causes an increase in q_Z. Consequently, hr^{max} decreases from combined action with the effect of changing in q(n) and q_Z(n).

The main conclusion from this graph is that **a decrea se in β leads to a greater h_r^{max} and a larger disturban ce rejection in Virtual Slope Walking**. However, β is a lways restricted by the physical parameters of the real ro bot.

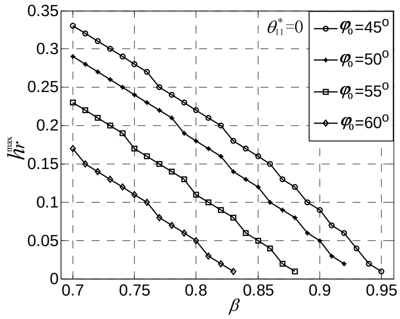

Fig. 4 Trajectory of maximum relative step height h_r^{max} versus length shorten ratio β

2.2 Effect of the Equivalent Extension Angle θ^*_{II}

The maximum relative step height h_r^{max} is shown as a function of θ^*_{II} in Fig. 5 with two values of β and φ_0 respectively. Fig. 5 shows a second order relationship between h_r^{max} and θ^*_{II}. As θ^*_{II} approaching zero from both side, h_r^{max} increases and reaches a maximum value at θ^*_{II} =0°. The vertical projection of leg length extension increases as θ^*_{II} approaching zero, and more potential energy is complemented. As a consequence, $q(n)$ and h_r^{max} increase while $q^z(n)$ stays constant. The vertical projection of leg length extension reaches its maximum at θ^*_{II} =0°.

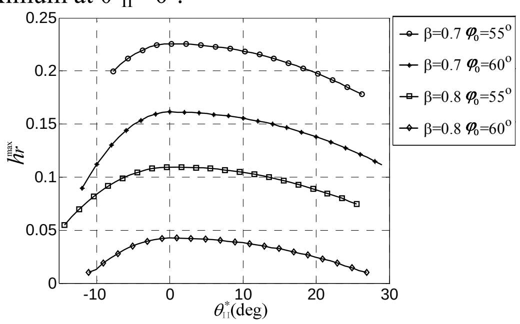

Fig. 5 Trajectory of maximum relative step height h_r^{max} versus equivalent extension angle θ^*_{II}

It can be concluded from this graph that **extending the stance leg more close to mid-stance will result in a greater h_r^{max} and a larger disturbance rejection in Virtual Slope Walking.** We can extend this conclusion to the Trajectory Leg Extension (TLE) that the extension phase being close to mid-stance also produces larger disturbance rejection.

2.3 Effect of the Inter-leg Angle φ0

The maximum relative step height h_r^{max} is shown as a function of φ_0 in Fig. 6 with four values of β. As shown in Fig. 6, h_r^{max} decreases with an increase in φ_0. The dissipation energy E_r increases as φ_0 increases. As a consequence, the system kinematic energy decreases, and $q(n)$ decreases. On the other side, an increase in φ_0 causes an increase in q^z. Consequently, h_r^{max} decreases from combined action with the effect of changing in $q(n)$ and $q^z(n)$.

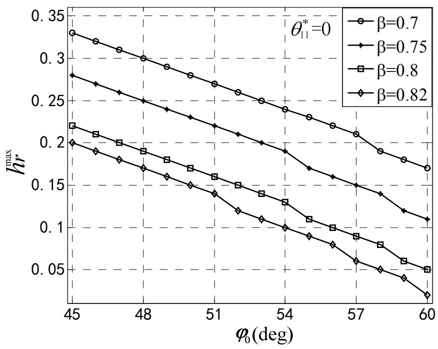

Fig. 6 Trajectory of maximal relative step height hrmax versus inter-leg angle φ_0

So we can conclude from this graph that **a smaller φ_0 results in greater h_r^{max} and a larger disturbance rejection in Virtual Slope Walking.**

2.4 Adjoint Relationship between the Walking Speed and Disturbance Rejection

The walking speed described by the Froude Number F_r is also determined by the model parameters β, θ^*_{II}, and φ_0 [16]. Therefore, as the model parameters change, there exists an adjoint relationship between the walking speed and disturbance rejection. The maximum relative step height h_r^{max} is shown as a function of F_r in Fig. 7.

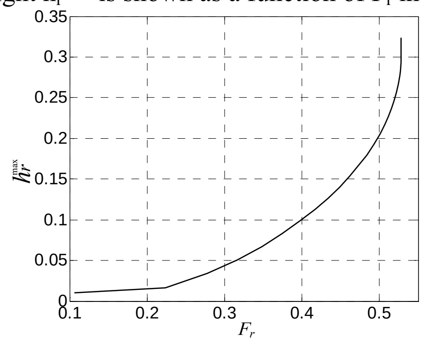

Fig. 7 Trajectory of maximal relative step height hrmax versus walking speed F_r

It is indicated from Fig. 7 that h_r^{max} increases with an increase in Fr. Since the effect of model parameters on h_r^{max} is the same as that on Fr, this conclusion exists distinctly. Such conclusion suggests that achieving fast walking speed always accompanying with large disturbance rejection.

From the above analyze results, it can be concluded that the performance of disturbance rejection in Virtual Slope Walking can be determined by the model parameters β, θ^*_{II}, and φ_0, which will be confirmed in the following experiment results.

Ⅴ. Experiment

1. Planar Bipedal Robot Stepper-2D

We use the planar bipedal robot Stepper-2D as a test bed of disturbance rejection in Virtual Slope Walking under single step perturbation. As shown in Fig. 8, Stepper-2D is mounted on a boom to constrain the body motion in the sagittal plane. The boom has three orthogonal DOF and the length is six times more than the height of the robot, so its effect on the robot sagittal movement can be ignored. Stepper-2D's leg length is 250mm and hip mass is 390g.

Fig. 8 Planar Bipedal Robot Stepper-2D with Point Foot.

The leg with the point foot is actuated in the hip and knee joint by digital servo motors. The telescopic leg motion is realized by bending and unbending the knee joint. And the swing leg motion is achieved by hip motor actuation [15]. All digital servo motors are controlled by a computer through serial bus.

2. Experimental Results

Stepper-2D successfully recovers from a maximum single step perturbation of 25mm in height, with a maximum relative step height h_r^{max} of 10% leg length. The hip and knee joints data from the motor sensors in the real walking experiment. Fig.9&10 presents the image sequences of the walking experiment under a single step-up and step-up-down perturbation of Stepper-2D respectively. The robot reaches the periodic state after several steps. And when the step height is greater than 25mm, it falls backward.

All the videos about the walking experiments including the single step-up and step-up-down could be found on our website http://v.youku.com/v_show/id_XMjA3ODM5OTcy.html.

Fig. 9 Image sequence extracted from video of a single step-up perturbation experiment (h_r^{max}=25mm)

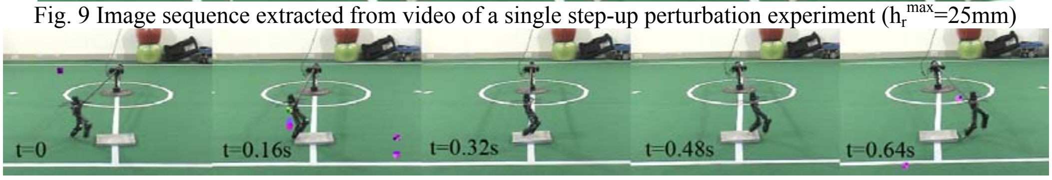

Fig. 10 Image sequence extracted from video of a single step-up-down perturbation experiment (h_r^{max}=25mm)

The compararison of maximum relative step height of Stepper-2D with other typical dynamic walkers is shown in table 1, suggesting that Stepper-2D achieves an improvement on the disturbance rejection of the previous research.

Table 1 Compararison of maximum relative step height

Type of dynamic walker	Maximum Relative Step Height
Stepper-2D	10%
Flaminge [17]	9%
Runbot [18]	4%
Mike [15]	2%

VI Conclusion and Future Work

In this paper, we analytically study the disturbance rejection of Virtual Slope Walking by introducing the ground step perturbation. We theoretically prove that ground step perturbation can be transformed to the disturbance of initial system state and the successful step handling walking comes from the system's cyclic stability. We then obtain the necessary and sufficient condition of recovering from the step perturbation by analyzing the relationship between the system state and the minimum initial state in the transition phase. Finally, we illustrate the effect of leg length shorten ratio β, equivalent extension angle θ^*_{II} and inter-leg angle φ_0 on the maximum relative step height h_r, demonstrating that achieving fast walking speed always accompanying with large disturbance rejection in Virtual Slope Walking. The step handling walking experiment of Stepper-2D verifies the theoretical analysis results and presents an improvement on the disturbance rejection compared with the other current results.

Starting from the step handling walking under the open-loop condition without external sensing device in this paper, we will introduce the sensing data of the step perturbation and study the sensor-based powered walking from the kinematic energy complement viewpoint, aiming at obtaining larger disturbance rejection for Virtual Slope Walking in the future work.

Acknowledgement

This work was supported partially by the National Nature Science Foundation of China (No. 60875065) and Supported by State Key Laboratory of Robotics and System (HIT) (No. SKLRS2010-ZD-01).

REFERENCES

[1] McGeer, T., 1990a, Passive dynamic walking, International Journal of Robotics Research, 9(2), pp. 62–82.

[2] S. Collins, A. Ruina, R. Tedrake, et al. Efficient Bipedal Passive-Dynamic Walkers. Science, 307(5712):1082-1085, 2005.

[3] M. Wisse. Three additions to passive dynamic walking; actuation, an upper body, and 3d stability, in Proc., Int. Conf. on Humanoid Robots. Los Angeles, USA, 2004.

[4] D.G.E. Hobbelen, M. Wisse. Ankle Actuation for Limit Cycle Walkers. International Journal of Robotics Research, 27(6):709-735, 2008.

[5] Collins, S.H, Ruina, A. A Bipedal Walking Robot with Efficient and Human-Like Gait. In Proc. IEEE International Conference on Robotics and Automation, 18-22 April, pp. 1983- 1988, 2005.

[6] F. Asano, Zhi-Wei Luo. Energy-Efficient and High-Speed Dynamic Biped Locomotion Based on Principle of Parametric Excitation, IEEE Trans. Robot., vol. 24, no. 6, pp. 1289–1301, 2008.

[7] Toyoyuki Honjo, Zhi-Wei Luo, Akinori Nagano. Parametric excitation of a biped robot as an inverted pendulum," Proceedings of IEEE/RSJ 2008 International Conference on Intelligent Robots and Systems, pp. 3408-3413, 2008.

[8] Yuji Harata, Fumihiko Asano, Kouichi Taji and Yoji Uno. Parametric excitation walking for four-linked bipedal robot, Proceedings of the 9th International IFAC Symposium on Robot Control (SYROCO), pp. 589-594, 2009.

[9] Mingguo Zhao, Ji Zhang, Hao Dong, Yu Liu, Liguo Li, and Xuemin Su. Humanoid Robot Gait Generation Based on Limit Cycle Stability, In the proceedings of the RoboCup Symposium, China, JUL 15-18, 2008.

[10] Hao Dong, Mingguo Zhao, Ji Zhang, Naiyao Zhang. Hardware design and gait generation of humanoid soccer robot Stepper-3D. Robotics and Autonomous Systems, 57:828-838, 2009.

[11] D. G. E. Hobbelen, M. Wisse. A Disturbance Rejection Measure for Limit Cycle Walkers: The Gait Sensitivity Norm. IEEE TRANSACTIONS ON ROBOTICS, VOL. 23, NO. 6, pp.1213-1224, 2007.

[12] M. Wisse. J. van Frankenhuyzen. Design and construction of mike; a 2d autonomous biped based on passive dynamic walking. Proc. Con f. Adaptive Motion of Animals and Machines. Kyoto, Japan: AMAM, 2003.

[13] Pratt J. Exploiting Inherent Robustness and Natural Dynamics in the Control of Bipedal Walking Robots. PhD Thesis, Massachusetts Institute of Technology, 2000.

[14] Geng T, Porr B, Wörgötter F. Fast biped walking with a sensor driven neuronal controller and real time online learning. International Journal of Robotics Research, vol. 25 no. 3: 243 -259, 2006.

[15] Hao Dong, Mingguo Zhao, Naiyao Zhang. High Speed and Energy Efficient Biped Locomotion Based on Virtual Slope Walking. Autonomous Robots, 2009.

[16] Mingguo Zhao, Hao Dong, and Naiyao Zhang. The Instantaneous Leg Extension Model of Virtual Slope Walking, In Proceedings of the IEEE/RSJ International Conference on Intelligent Robots and Systems, 2009.